Tunable resonant light propagation through 90° bend waveguide based on strained photonic crystal

2004 J. Phys.: Condens. Matter 16 1523

(http://iopscience.iop.org/0953-8984/16/9/001)

INSTITUTE OF PHYSICS PUBLISHING JOURNAL OF PHYSICS: CONDENSED MATTER

J. Phys.: Condens. Matter **16** (2004) 1523–1530 PII: S0953-8984(04)68884-9

Tunable resonant light propagation through 90° bend waveguide based on strained photonic crystal

Natalia Malkova

Materials Research Institute, Pennsylvania State University, University Park, PA 16802, USA

Received 12 September 2003, in final form 5 January 2004
Published 20 February 2004
Online at stacks.iop.org/JPhysCM/16/1523 (DOI: 10.1088/0953-8984/16/9/001)

Abstract

The degenerate state in two-dimensional photonic crystal is studied. The photonic analogue of the static Jahn–Teller effect is utilized for realizing tunable propagation through photonic crystal waveguide bends. It is shown that the resonant coupling of the photon modes at the corner can be tuned by the symmetry and magnitude of the distortion of the lattice.

(Some figures in this article are in colour only in the electronic version)

Photonic crystals are of importance for numerous applications involving light modulation [1]. One such useful system based on photonic crystals is the high-Q photonic bandgap resonant cavity that can be realized by introducing a point defect into an otherwise regular photonic lattice, which induces the existence of exponentially decaying states that appear within the bandgap. Although the modes of each cavity were tightly confined at the defect sites, overlap between the nearest-neighbour modes is enough to provide the propagation of photons via hopping. The guiding and bending of the electromagnetic wave through highly localized defect modes in a photonic crystal was reported by Bayidir *et al* [2]. The most important feature of these coupled cavity waveguides is the possibility of constructing lossless and reflectionless bends [3, 4]. This ability has a crucial role in overcoming the problem of guiding light around sharp corners in the optical circuits [5]. It is worth noting that the high efficiency of the sharp corner photonic crystals waveguide is, to some extent, similar to the behaviour of discrete solitons in nonlinear waveguide arrays [6].

On the other hand, for application in optical devices, it is important to realize the tunability of the photonic crystals. A tunable light propagation in Y-shaped waveguides has been recently reported [7] based on two-dimensional photonic crystals with triangular lattices using liquid crystals as the linear defect. In this paper we propose to use a tunable splitting of the degeneracy of the defect state, for tuning the defect mode coupling at the corner of the coupled cavity waveguide. The effect that we exploit is analogous to the Jahn–Teller effect in solids [8]. It is based on the symmetrical analysis of the splitting of degenerate states by a convenient distortion of the lattice. In our recent paper [9], we have reported that, in photonic crystals subject to lattice distortions, the Jahn–Teller phase transition can be observed if the system

satisfies the critical conditions. The aim of this paper is to show an application of the photonic analogue of the static Jahn–Teller effect for the design of tunable coupled cavity waveguides.

When studying the Jahn–Teller effect in solids, we consider a crystal subject to phonon vibrations. In application to photonic crystals, this problem is reduced to studying the defect photonic crystal subject to mechanical vibrations of the lattice [9]. In this paper we limit ourselves to studying the photonic crystal under static distortion of the lattice. As a model material, we consider a two-dimensional square photonic lattice doped by the defect rods. The point group symmetry of the square lattice is C_{4v}. If the defect rod is localized at the site of the lattice, then by symmetry it may be described both by one-dimensional $A_{1,2}$, $B_{1,2}$ and two-dimensional E irreducible representations of the group C_{4v} [10]. One-dimensional irreducible representations result in a non-degenerate photon state. The two-dimensional representation results in a doubly degenerate state represented by the two 1×2 column basis vectors having the shape of the p_x and p_y orbitals [10]. We are going to study the splitting of the degeneracy of this state.

Our problem now is to find such a perturbation V of the distortion of the lattice, which results in splitting the doubly degenerate E state. For the two-dimensional photonic crystal, the eigenvalue problem for the E or H polarization is [11]

$$(H_0(\mathbf{r}) + V(\mathbf{r}))\Psi(\mathbf{r}) = \frac{\omega^2}{c^2}\Psi(\mathbf{r}). \tag{1}$$

In the first order of perturbation theory, the solution for the eigenfunction should be presented as $\Psi(\mathbf{r}) = \sum_{i=x,y} A_i p_i(\mathbf{r})$, where A_i are unknown coefficients. The unperturbed Hamiltonian H_0 has the symmetry of the simple square lattice, with the solution $H_0|p_i\rangle = \frac{\omega^2}{c^2}|p_i\rangle$ giving the doubly degenerate state with the eigenvalue $\omega = \omega_0$.

Following the analysis in [9], we can present all distortions of the lattice in terms of the normal coordinates as a sum of the normal irreducible distortions $\mathbf{R}_\alpha$. Then in the first approximation, with respect to the magnitude of the lattice distortion, the perturbation can be extended over normal symmetrized displacements $V(\mathbf{r}) = \sum_\alpha \mathbf{R}_\alpha \cdot \frac{\partial V^\alpha}{\partial \mathbf{r}}|_0$, where the deformation potential $\frac{\partial V^\alpha}{\partial r}$ is calculated at the zero lattice distortion [12]. In the case of the two-dimensional square lattice with the defect in the site of the lattice, there are allowed $2A_1$, B_1, $2B_2$ and $2E$ normal irreducible distortions of the lattice. The A_1 perturbation is a total symmetrical one, while B_1 and B_2 are antisymmetrical normal distortions described by the one-dimensional irreducible representations. The E distortion is characterized by the two-dimensional irreducible representations with the 1×2 basis vector, the components transforming into each other [12].

As follows from the Jahn–Teller theorem [12], to split the doubly degenerate E photonic state the matrix element of the corresponding perturbation $V_{ij}^\alpha = \int p_i(\mathbf{r}) V^\alpha(\mathbf{r}) p_j(\mathbf{r})\, d\mathbf{r} \neq 0$. From the symmetry analysis, this matrix element is nonzero if and only if $E \times E = \alpha$. Since $E^2 = A_1 + A_2 + B_1 + B_2$, only perturbations with the symmetry of the A_1, B_1 and B_2 distortions can shift the degeneracy of the E defect mode.

It is obvious that the interaction of the defect photon state with the total symmetrical distortion A_1 results in equal shifts each of the level of the doubly degenerate state without lifting the degeneracy. The non-symmetrical $B_{1,2}$ perturbations can only split the degenerate photon state. For the B_1 distortion, $V_{xx}^{B_1} = -V_{yy}^{B_1}$ and $V_{xy}^{B_1} = 0$. As a result, the degeneracy of the E-photonic mode is removed, resulting in two levels $\omega_{1,2}^{B_1} = \omega_0 \pm V_{xx}^{B_1}$, being described by the eigenvectors with the p_x and p_y symmetries. For the B_2 distortion, $V_{xx}^{B_2} = V_{yy}^{B_2} = 0$ and $V_{xy}^{B_2} = V_{xy}^{B_2}$. This result in the two split $|p_x \pm p_y\rangle$ orbitals with the energy $\omega_{1,2}^{B_2} = \omega_0 \pm V_{xy}^{B_2}$.

What follows from this analysis? First, by choosing the perturbation, we can control the symmetry of the split states. So the B_1 perturbation should be applied to the system if we want

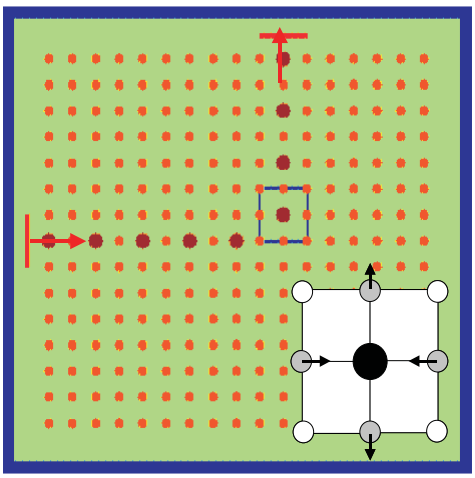

Figure 1. The structure studied of the coupled cavity 90° bend waveguide with the corner unit cell distorted by the B_1 perturbation, as shown in the inset.

to get $|\mathrm{p}_x\rangle$ and $|\mathrm{p}_y\rangle$ symmetries of the split states. By means of the B_2 perturbation, we will get the $|\mathrm{p}_x \pm \mathrm{p}_y\rangle$ split states. Second, because of the linear dependence of the perturbative potential on the amplitude of the distortion ($V_{ij}^{\alpha} \sim |\mathbf{R}_\alpha|$), the splitting of the doubly degenerate level should show a linear scaling $\Delta\omega \sim v^{\alpha}\Delta r$ with the magnitude of the distortion of the lattice, $|R_\alpha| = \Delta r$, through the deformation potential, v^{α}, as a scaling coefficient. Numerical support for this conclusion has been presented in [9], where the splitting of the degenerate state in the one-defect photonic crystal had been studied by means of the supercell technique and finite difference time domain (FDTD) simulations. We emphasize that the analysis presented allows one to select the perturbation of the lattice, resulting in a desirable magnitude and symmetry of the defect state splitting. Therefore, we can tune the splitting of the defect mode both by frequency and by symmetry.

We turn now to study the coupled cavity 90° bend waveguide shown in figure 1. This system consists of two branches. Here we take the reference system such that the first waveguide branch (before bending) is directed along the x axis (x branch), and the second branch (after bending) is directed along the y axis (y branch). To specify the parameters of the crystal we consider a square photonic crystal of the dielectric rods, embedded in air, with lattice constant a, radius of the rods $r = 0.2a$ and dielectric constant $\epsilon_{\mathrm{r}} = 11.9$. Here, only modes with odd (TM-like) symmetry are considered, since that is the symmetry of the bands exhibiting a gap for the square lattice [13]. We study the defect state created by the defect rod with radius $r_{\mathrm{d}} = 0.3a$ and the same dielectric constant $\epsilon_{\mathrm{d}} = 11.9$ as the other rods, because such a defect gives the doubly degenerate E defect state inside the first bandgap [9]. This is the state that we will now examine.

In order to tune the propagation of the light through the system we place at the corner the so-called Jahn–Teller cell which is magnified in the inset of figure 1. From the geometry of this system, we immediately guess that the best coupling between the two branches of the coupled cavity waveguide will be achieved if we can control the splitting of the $|\mathrm{p}_x\rangle$ and $|\mathrm{p}_y\rangle$ states of the corner defect. Because of this, the corner Jahn–Teller cell should be distorted by the B_1 perturbation. We consider distortions of the lattice in the limits $\Delta r = 0 - 0.3a$, keeping in mind that only small distortions ($\Delta r \ll a$) allow for the validity of the linear approximation of the perturbative potential.

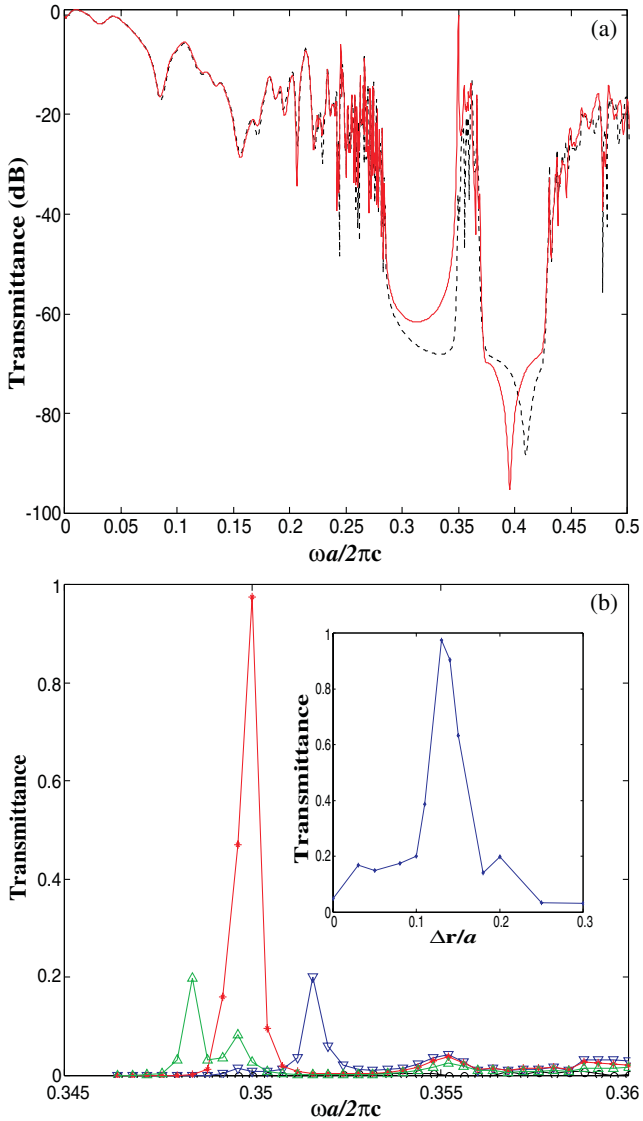

Figure 2. Computed transmission coefficient of the structure with $\Delta r/a = 0$ (broken curve) and 0.13 (full curve) (a). The relative transmission intensity inside the bandgap for the structures with $\Delta r/a = 0$ (line with open circles), 0.10 (line with open inverted triangles), 0.13 (line with stars) and 0.2 (line with open triangles) (b). The inset shows the relative transmission intensity as a function of the lattice distortion.

To analyse this structure, we use the FDTD simulations, following the technique described in [14]. Our computational domain is shown in figure 1. It contained 15×17 unit cells. Each unit cell was divided into 20×20 discretization grid cells. The computational domain was surrounded by perfect matched layers, with the thickness corresponding to 10 layers of the discretization grid. The time step was taken equal to $\Delta t = 1/(2\Delta xc)$ to satisfy the convergence of the FDTD technique. The numerical simulations were performed with the total number of time steps equal to 100 000 and 200 000 in order to check if the stationary regime of the FDTD

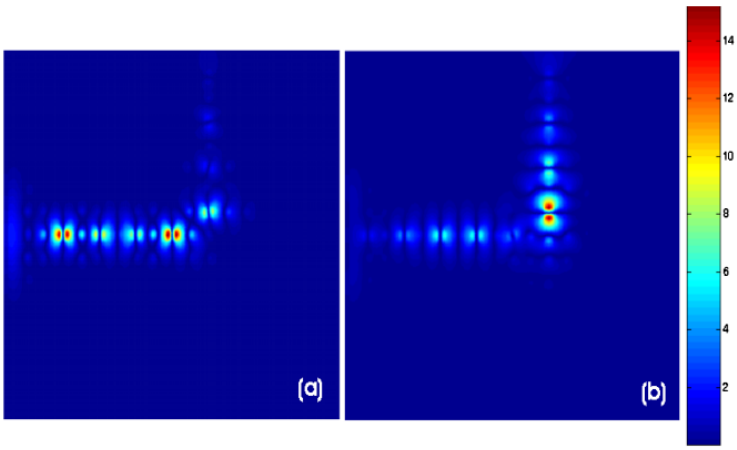

Figure 3. Pattern of the z component of the electric field in the frequency domain for the resonant frequency $\omega = 0.349$ at $\Delta r/a = 0$ (a) and 0.13 (b).

simulations is reached. The source was simulated as a Gaussian beam in time domain and in the coordinate space with the width of the beam equal to 40 grid cells. To analyse the transmission of the structure we collected the signal at the output of the waveguide structure and compared these data with the reference signal collected at the input of the structure, as described in [15].

We observed an increase of the light transmission when $\Delta r > 0$. This distortion is shown in the inset of figure 1. The transmission decreases at $\Delta r < 0$, which is the case of the oppositely directed distortion. The computed transmission coefficient of the structure with $\Delta r/a = 0$ (broken curve) and 0.13 (full curve) is presented in figure 2(a). Figure 2(b) shows the relative transmission intensity inside the bandgap for the structures with $\Delta r/a = 0, 0.10, 0.13, 0.20$. From these data, we note that the transmission of the structure is very frequency selective with the width of the transmission peak $\delta\omega \sim 10^{-3}$ (in relative units). The transmission coefficient of the structure as a function of the lattice distortion, presented in the inset of figure 2(b), shows the resonant behaviour with the sharp maximum at $\Delta r/a = 0.13$. Figures 3(a) and (b) present the pattern of the z component of the electric field in the frequency domain for the resonant frequency $\omega = 0.349$ at $\Delta r/a = 0$ and 0.13, respectively.

We will analyse this system in terms of the tight-binding model [2]. In the first approximation, the doubly degenerate state of the linear n-site chain generates the two bands $\omega_\parallel = \omega_0 \pm \beta_\parallel$ and $\omega_\perp = \omega_0 \pm \beta_\perp$. Here $\beta_\parallel$ is the coupling coefficient between the $|p_x\rangle$ (or $|p_y\rangle$) states at the x (or y) branch, and $\beta_\perp$ is the coupling coefficient between the $|p_y\rangle$ (or $|p_x\rangle$) at the x (or y) branches. In figure 4, the supercell plane-wave calculations show the band spectrum of each waveguide branch (a), as well as the Poynting vectors for the $\omega_\parallel$ (b) and $\omega_\perp$ (c) bands at the point (0, 0) of the supercell Brillouin zone. The band $\omega_\parallel$ is characterized by the symmetry of the p orbitals parallel and directed along the defect chain, that is $|p_x\rangle$ for the x branch and $|p_y\rangle$ for the y branch. The band $\omega_\perp$ is characterized by the orthogonal, with respect to the first band, p orbital, that is the $|p_y\rangle$ and $|p_x\rangle$ orbitals for the x and y branches, respectively. Because of the much smaller coupling between the $|p_y\rangle$ states than the $|p_x\rangle$ states at the x branch, $\beta_\perp < \beta_\parallel$. From the width of the bands $\omega_\parallel$ and $\omega_\perp$ shown in figure 4, we can estimate for the defect crystal studied, $2\beta_\perp = 0.002$ and $2\beta_\parallel = 0.01$. It is of importance for the linear chain with a finite number of n sites that the spectrum of each band consists of the n levels distant at $\sim 2\beta_{\parallel(\perp)}/(n-1)$.

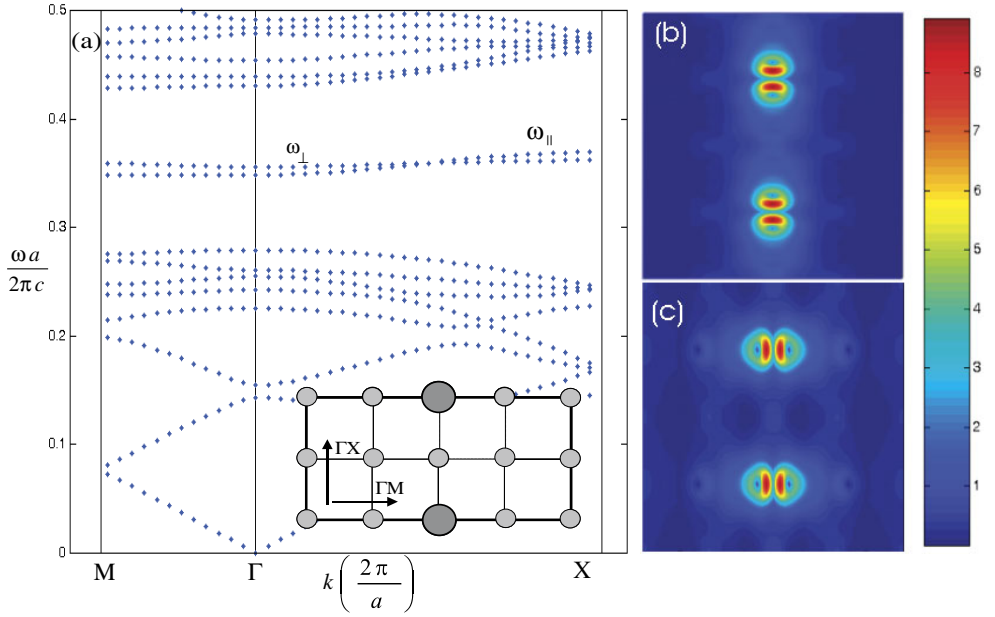

Figure 4. (a) Supercell plane-wave calculation of the band spectrum of the supercell, shown in the inset, which presents the spectrum of each waveguide branch. Distribution of the Poynting vector for $\omega_\parallel$ (b) and $\omega_\perp$ (c) bands, calculated at the point (0, 0) of the supercell Brillouin zone.

It is obvious that the strongest coupling of the cavity modes, and consequently the highest transmission, will be in the case when the light propagates through the $|p_x\rangle$ states along the x branch before the bend and through the $|p_y\rangle$ states along the y branch after bending. However, from figure 4(a) we note the distance between the two bands, $\omega_\parallel$ and $\omega_\perp$, is small and, moreover, for some selective wavevectors these bands overlap. Because of this, the light can tunnel at the corner from the band $\omega_\parallel$ to the band $\omega_\perp$, without flipping the symmetry. But in such a case a lot of energy is not transmitted across the corner, firstly, during the tunneling and, secondly, because of a bad coupling between the p_x modes after bending. The pattern of the E_z field, shown in figure 3(a), provides evidence that such a propagation of the light is preferable in the case of $\Delta x = 0$. As a result, the transmission of such a structure will be small (broken curve in figure 2(a)).

Now, if the corner cell is distorted by the B_1 perturbation, the $|p_x\rangle$ and $|p_y\rangle$ states of the corner defect are separated by $\Delta\omega = 2V^{B_1} = v^{B_1}\Delta r$. The deformation constant can be easily found from the supercell calculations of the defect level splitting, presented in figure 4(a) of [9]. For the B_1 perturbation, $v^{B_1} \sim 0.1$.

The transmission coefficient of the structure increases as soon as $\Delta r > 0$, being at the maximum at $\Delta r v^{B_1} \sim 2\beta_\parallel$. The reason for this is that the magnitude of the defect level splitting is governed by the magnitude and symmetry of the lattice distortion. For the distortion shown in the inset of figure 1, the $|p_x\rangle$ state of the corner defect shifts up in energy, while the $|p_y\rangle$ states goes down, and vice versa for the opposite directed distortion. If the $|p_x\rangle$ state of the corner defect goes up in frequency, this results in lowering the probability for tunnelling through this state without flipping the symmetry. If simultaneously the $|p_y\rangle$ state goes down, coming closer to the highly transmitted levels for each of the waveguide branches, then the transmission through the corner should increase. However, for the small distortion of the lattice such that

$\Delta r v^{B_1} \ll \beta_\parallel$, the effect of the lattice distortion on the spectrum of the y branch is small. The band spectrum will be still governed by the coupling parameter β, with the wavefunctions being linear combinations of the all-defect states localized at each of the sites. When $\Delta r \geqslant 2\beta_\parallel / v^{B_1}$ the corner defect within the distorted Jahn–Teller cell becomes independent of the other defects of the y branch, resulting in a resonance defect state. Its spectrum will be mostly governed by the lattice distortion, giving the level with the strongly localized wavefunction. The resonant transmission of the structure is observed when the $|\mathrm{p}_y\rangle$ state of the corner defect is matched by frequency with the lowest level of the p_x band of the x branch, $\omega_\parallel^{\mathrm{m}} = \omega_0 - \beta_\parallel$. The frequency of the distorted E states of the corner defect is equal to $\omega_{1,2}^{\mathrm{c}} = \omega_0 \pm v^{B_1} \Delta r/2$. Then the resonant condition $\omega_{1,2}^{\mathrm{c}} = \omega_\parallel^{\mathrm{m}}$ gives $\Delta r v^{B_1} = 2\beta_\parallel$. The width of the resonant peak is determined by the width of the split $|\mathrm{p}_y\rangle$ corner defect state. Taking the value $2\beta \sim 0.01$, we find that the resonance should be observed at $v^{B_1} \Delta r \sim 0.01 > 0$. Using the known value $v^{B_1} \sim 0.1$, we find that this splitting corresponds to the distortion of the lattice $\Delta r/a \sim 0.1$, in reasonable agreement with the FDTD experiment. From figure 2(b) we can follow how the $|\mathrm{p}_y\rangle$ split state of the corner defect moves when we change the lattice distortion. In the case of the opposite directed distortion $\Delta r < 0$, the $|\mathrm{p}_x\rangle$ and $|\mathrm{p}_y\rangle$ states shift in opposite directions as well. As a result, the transmission coefficient of the structure decreases. The pattern of the E_z field for $\Delta r/a = 0.13$ at the resonant frequency $\omega = 0.349$ presented in figure 3(b) provides support for this analysis.

It is worth mentioning that we have considered here the concrete structure with the given number of defects for both waveguide branches. This geometry of the structure determines the resonant frequency of the transmission peak and the required distortion of the corner cell for the resonant coupling between the two branches. By changing the number of sites in each of the branches, we can tune the resonant transmission frequency.

In conclusion, in this paper we have shown the application of the static Jahn–Teller effect for tuning light propagation through a 90° bend coupled cavity waveguide based on a two-dimensional photonic crystal. The structure with working B_1 perturbation has been considered. The propagation of the light has been shown to be characterized by the resonant behaviour as a function of the lattice distortion, with the sharp maximum corresponding to the best energy and symmetry coupling between the two branches. The width of the transmission peak is determined by the width of the split corner defect state. As a result, the transmission coefficient of the structure is very frequency-selective with the width of the transmission peak $\sim 10^{-3}$ (relative units). For the waveguide devices operating at the light wavelength 1.55 μm, this corresponds to the width of the transmission peak $\sim$2 nm. In this paper we were dealing with the static Jahn–Teller effect only. For straightforward implementation of the effect it could be suggested to construct a photonic crystal on the piezoelectric substrate, giving a needed distortion of the lattice near the defect [16, 17]. However, more exciting opportunities will be opened up in the case of the realization of the dynamic Jahn–Teller effect, resulting in a spontaneous phase transition of the corner Jahn–Teller cell. I believe that the flexibility of the photonic structures, studied in the present paper, will draw attention to the idea of the phase transition in photonic crystals.

Acknowledgments

I would like to acknowledge the support from the Center for Collective Phenomena in Restricted Geometries (Penn State MRSEC) under NSF grant DMR-00800190 and National Science Foundation grant ECS-9988685. I thank the Materials Simulation Center (Penn State) for provision of the computer facilities.

References

[1] Soukoulis C M (ed) 2001 *Photonic Crystals and Light Localization in the 21st Century* (*NATO Science Series* vol 563) (Dordrecht: Kluwer–Academic)
[2] Bayidir M, Temelkuran B and Ozbay E 2000 *Phys. Rev.* B **61** R11855
Bayidir M, Tanriseven S and Ozbay E 2001 *Appl. Phys.* A **72** 117
[3] Yariv A, Xu Y, Lee R K and Scherer A 1999 *Opt. Lett.* **24** 711
[4] Stefanou N and Modinos A 1998 *Phys. Rev.* B **57** 12127
[5] Mekis A, Chen J C, Kurland I, Fan S, Villeneuve P R and Joannopoulos J D 1996 *Phys. Rev. Lett.* **77** 3787
[6] Christodoulides D N and Eugenieva E D 2001 *Phys. Rev. Lett.* **87** 233901
[7] Takeda H and Yoshino K 2003 *Phys. Rev.* B **67** 073106
[8] Landau L D and Liphshitz E M 1974 *Quantum Mechanics* (Moscow: Nauka)
[9] Malkova N, Kim S and Gopalan V 2003 *Phys. Rev.* B **68** 045105
Malkova N, Kim S and Gopalan V 2003 *J. Phys.: Condens. Matter* **15** 4535
[10] Sakoda K and Shiroma H 1997 *Phys. Rev.* B **56** 4830
[11] Maradudin A A, Kuzmiak V and Mcgurn A R 1996 *Photonic Band Gap Materials* ed C M Soukoulis (Dordrecht: Kluwer–Academic) pp 271–318
[12] Bersuker I B 1983 *The Jahn–Teller Effect and Vibronic Interactions in Modern Chemistry* (New York: Plenum)
[13] Malkova N, Kim S and Gopalan V 2002 *Phys. Rev.* B **66** 115113
[14] Taflove A and Hagness S C 2000 *Computational Electrodynamics: the Finite-Difference Time-Domain Method* (Boston, MA: Artech House Publishers)
[15] Talneau A, Le Gouezigou L, Bouadma N, Kafesaki M and Soukoulis C M 2002 *Appl. Phys. Lett.* **80** 547
[16] Kim S and Gopalan V 2001 *Appl. Phys. Lett.* **78** 3015
[17] Malkova N, Kim S and Gopalan V 2003 *Appl. Phys. Lett.* **83** 1509